Energy storage in the primary photoproduct of vision

Bifone, A.; Groot, H.J.M. de; Buda, F.

Energy Storage in the Primary Photoproduct of Vision

Angelo Bifone,† Huub J. M. de Groot,† and Francesco Buda*,‡

Leiden Institute of Chemistry, Gorlaeus Laboratoria, University of Leiden, 2300 RA Leiden, The Netherlands, and Istituto Nazionale per la Fisica della Materia, Laboratorio Forum, Scuola Normale Superiore, Piazza dei Cavalieri 7, I-56126 Pisa, Italy

Received: July 31, 1996; In Final Form: November 18, 1996[⊗]

We present a Car−Parrinello *ab-initio* molecular dynamics study of rhodopsin, the membrane protein responsible for the first step in vision. The ground state structures of the retinylidene chromophores of rhodopsin and of its primary photoproduct, bathorhodopsin, have been calculated with a simulated annealing procedure. In bathorhodopsin, the energy is primarily stored in distortions of the conjugated backbone of the chromophore, which presents a highly strained all-*trans* configuration. The roles of steric and electrostatic chromophore−protein interactions in the energy storage mechanism are discussed. An analysis of the HOMO and LUMO charge distributions in rhodopsin and bathorhodopsin has been performed.

I. Introduction

The primary event in the process of vision involves the photoconversion of a seven-helix membrane protein, rhodopsin, to a metastable intermediate, bathorhodopsin.[1,2] The chromophore of rhodopsin consists of an 11-*cis* retinylidene prosthetic group linked to a lysine protein residue (Ly 296) via a protonated Schiff base (PSB) (Figure 1). The absorption of a photon induces the isomerization of the 11-*cis*-retinal chromophore to an all-*trans* form in bathorhodopsin. This photoprocess is completed in about 200 fs, in the fastest photochemical reaction known[3] and is characterized by a quantum yield of 65%.[4] At physiological temperatures, the primary photoproduct, bathorhodopsin, quickly decays through several subsequent photointermediates and eventually dissociates into all-*trans*-retinal and opsin. This process initiates a chain of biochemical reactions that lead to the closing of the sodium channels in the cell membranes. At temperatures < 130 K, bathorhodopsin is stable.[5] Photocalorimetric studies have shown that ∼32 kcal/mol are stored in bathorhodopsin trapped at 77 K.[6,7] The energy conversion process in the primary event is remarkably efficient, since ∼60% of the energy of the absorbed photon is stored in the primary photoproduct.

Several mechanisms for the energy storage in bathorhodopsin have been proposed. Honig and co-workers[8] suggested that charge separation between the positively charged PSB and its negative counterion (Glu 113) upon photoisomerization is the main mechanism. Distortions of the conjugated backbone may also account for the 32 kcal/mol stored in bathorhodopsin.[9] A combination of these two mechanisms has been proposed by Birge and co-workers,[10] who conclude that conformational distortions of the chromophore account for 60% of the energy stored, while 40% can be attributed to charge separation between the chromophore and the counterion. ^{13}C magic angle spinning NMR experiments have shown no substantial difference between the electronic charge distributions in the chromophores of rhodopsin and bathorhodopsin and exclude charge separation between the chromophore and the counterion as a significant mechanism for energy storage.[11]

In this paper we present a Car−Parrinello *ab-initio* molecular dynamics[12] study of the energy storage mechanism in a retinal protonated Schiff base (RPSB), including the relevant interactions with the protein and constraints on the structure of the RPSB in rhodopsin, which have been recently determined by solid state NMR.[13] Within the Car−Parrinello approach, the ground state equilibrium structure of the RPSB can be determined with a simulated annealing procedure, which allows overcoming local energy minima and flat regions on the Born−Oppenheimer hypersurface.

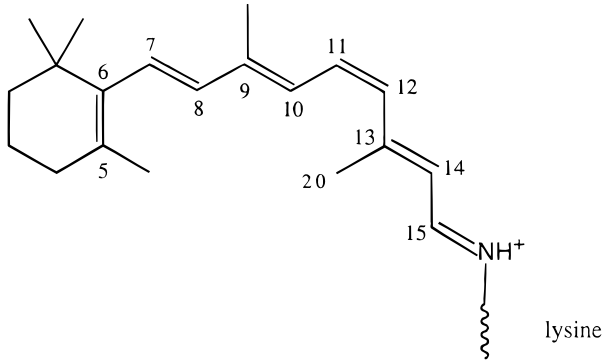

Figure 1. Schematic structure of the 11-*cis* protonated Schiff base of retinal, showing the conventional numbering system.

We show that the *cis-trans* isomerization of the chromophore leads to a highly strained all-*trans* form in bathorhodopsin, where the energy is mainly stored in torsional distorsions of the conjugated backbone. This configuration is obtained from the structure of the RPSB of rhodopsin with relatively small atomic displacements, compatible with the very short time of formation of the primary photoproduct. The structures of the rhodopsin and bathorhodopsin RPSB optimized with and without a model counterion have been compared to elucidate the role of the electrostatic interaction. We conclude that the electrostatic interaction with a counterion is crucial to the energy storage mechanism, since it locks the positive charge borne by the chromophore in the terminal region of the molecule, in agreement with the ^{13}C NMR data,[11] and increases the stiffness of the backbone.

II. Computational Methods

The *ab-initio* molecular dynamics approach describes the Newtonian dynamics of a system by using an interatomic potential obtained at each time step from the instantaneous

* Corresponding author (E-mail: buda@forum.sns.it).
† University of Leiden.
‡ Scuola Normale Superiore.
⊗ Abstract published in *Advance ACS Abstracts,* February 1, 1997.

S1089-5647(96)02339-5 CCC: $14.00

electronic ground state.[12] The electronic structure is obtained within the density functional theory (DFT) in the local density approximation (LDA)[14] using the Perdew and Zunger[15] parametrization of numerical quantum Monte Carlo results.[16] We have included gradient corrections (GC) to the exchange−correlation functional in the form proposed by Becke[17] and Perdew.[18] Density functional theory in local density approximation (DFT-LDA) studies of infinite conjugate chains have shown severe limits in the description of the dimerization.[19] However, we have recently shown that the Car−Parrinello method provides an excellent framework to study retinals[20] and rhodopsin.[21] In fact, in such short conjugated chains, the bond alternation is determined by the asymmetry of the molecule and is stabilized by the β-ionone ring, the side methyl groups, and the highly electrophylic tail.[20] Soft first-principles pseudopotentials[22] have been used to describe the interactions of the valence electrons with the inner cores. The Kohn−Sham single-particle wave functions are expanded on a plane wave basis set with an energy cutoff of 20 Ry. We have tested the convergence of the calculation relative to the energy cutoff on a C_2H_6 and a HCN molecule up to 30 Ry. At 20 Ry the C−C and C−N bond lengths are already close to the fully converged values within ∼1.0%. The C−C and the C−N stretch frequencies are accurate within ∼1.0% and ∼2.0%, respectively. The expansion in terms of plane waves implies the use of periodic boundary conditions. We have used a simulation box of 36 × 22 × 22 au, large enough to avoid interaction with the images. The time step for the molecular dynamics simulations is 0.15 fs.

III. A Model for the Chromophore of Rhodopsin

The interactions with the protein determine to a large extent the remarkable properties of the retinylidene chromophore of rhodopsin. Steric and electrostatic interactions with protein residues in the binding pocket affect the chromophore structure and its potential energy surface. At present, no high-resolution three-dimensional structure exists for rhodopsin and its chromophore. However, Raman spectroscopy and ^{13}C NMR have provided evidence for specific protein−chromophore interactions and constraints to the structure of the RPSB in the protein-binding pocket.[1,2]

Recently, solid state magic angle spinning NMR has been applied to high-precision distance measurements in rhodopsin and one of its photointermediates,[13] providing evidence for distortions of the retinal chromophore induced by the protein. In rhodopsin, the steric interaction of the methyl group bound to C13 with protein residues induces a twist of the C12−C13 bond and an out-of-plane distortion of the backbone. We have modeled the rhodopsin chromophore starting with initial C20−C11 and C20−C10 distances of 3.0 and 3.05 Å, respectively, as determined by the experiment.[13] The RPSB has been terminated with a $-CH_2-CH_3$ group to mimic the linkage of the chromophore to the protein lysine group.

The chromophore bears a net positive charge, as a result of the protonation of the retinal−lysine Schiff base. Two-photon absorption studies have shown that the binding site is neutral, which implies that a negative counterion is located in the vicinity of the chromophore.[23] Mutagenesis experiments show that the primary counterion is the glutamate protein residue Glu113,[24] Resonance Raman spectroscopy and NMR support the picture of a specific chromophore−counterion interaction in the region C12−C13.[25−28] We have modeled the counterion with a chlorine ion (Cl^-) placed at ∼4.0 Å from C12. This counterion is much simpler than the carboxylate group in the glutamate residue. However, semiempirical calculations have shown that this counterion captures the essential electrostatic interaction and yields a charge density distribution that is consistent with experiment.[27] For comparison, we have performed structure minimization without the counterion, in order to characterize the effects of the electrostatic interaction on the chromophore geometry and electronic structure.

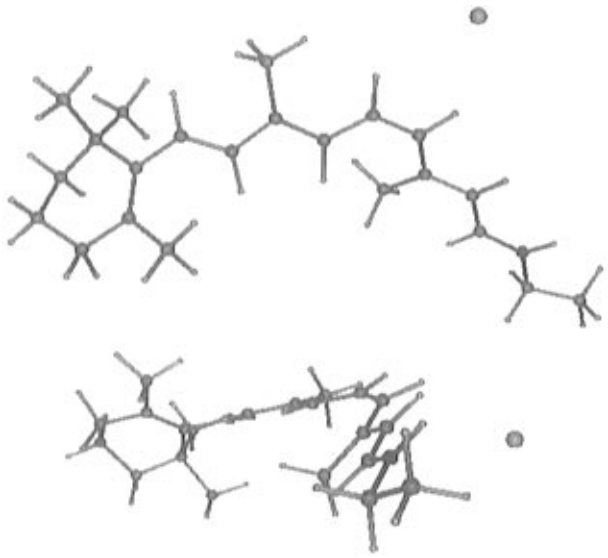

Figure 2. Equilibrium structure of the chromophore of rhodopsin including the experimental structural constraints. Parts a (top) and b (bottom) show the chromophore from two different points of view. The steric interactions with the binding pocket induce an out-of-plane deformation of the molecule, as evident in b. The nitrogen atom is indicated by the dark ball. The isolated ball is the Cl^- counterion.

Ultrafast optical spectroscopy[3] has shown that the primary photoproduct is formed in 200 fs. No dramatic rearrangement of the protein or of the chromophore structures can occur in such a short time interval. The time scale to rearrange the chromophore to a planar structure, which is the energy minimum configuration for an all-*trans* RPSB when no constraints are imposed, is much longer than the time of formation of bathorhodopsin.[1] Thus, the retinylidene chromophore of bathorhodopsin is not in a fully relaxed all-*trans* form. The structural changes from rhodopsin to bathorhodopsin have to be compatible with the short time scale of formation of the primary photoproduct.

Solid state NMR data have shown that the side methyl groups bound to C9 and C13 experience steric interaction with protein residues, thus supporting the idea of a tight binding pocket.[13] In our simulations, we have fixed in space the position of the carbon atoms of these methyl groups, to mimic the steric hindrance of the protein residues. Also the counterion and the terminal $-CH_2-CH_3$ group have been blocked, as no changes in the protein structure are expected in the short time of formation of bathorhodopsin.

IV. Ground State Structure

The ground state equilibrium structures of the RPSB of rhodopsin (Figure 2) and bathorhodopsin (Figure 3) have been calculated with a simulated annealing procedure. Starting from the initial geometry of the 11-*cis* RPSB, we let the system evolve freely for about 120 fs until an equilibrium temperature of about 70 K is reached. The temperature has been then gradually lowered to 5 K for a total simulation time of about 100 fs. Noticeably, a first attempt of structural optimization with a steepest descent algorithm has shown an extremely low rate of total energy decrease, thus revealing a fairly flat potential energy surface in the vicinity of the energy minimum. A simulated annealing procedure is very efficient when local gradients in

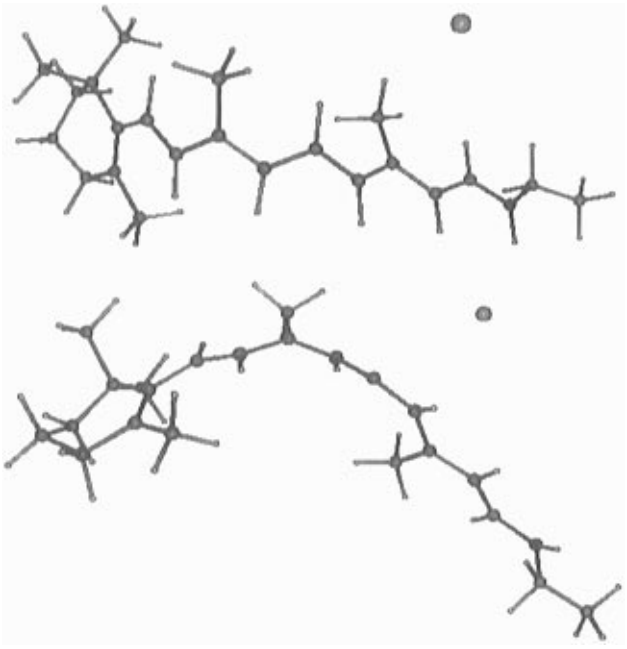

Figure 3. Structure of the chromophore of bathorhodopsin after simulated annealing from two different points of view. The chromophore presents an all-*trans* configuration (a, top). The structure is highly distorted (b, bottom). The strain is distributed in in-plane and torsional deformations along the entire backbone.

the Born−Oppenheimer surface are small and is crucial to determine the equilibrium structure of the RPSB. The C20−C11 and C20−C10 distances in rhodopsin after the optimization procedure are 3.05 and 3.08 Å, respectively, and do not substantially differ from the initial values. The carbon−carbon bond lengths along the backbone chain are reported in Table 1. The rhodopsin RPSB presents clear bond alternation, except for the terminal region close to the nitrogen atom. For comparison, we have also reported the carbon−carbon distances for a neutral Schiff base, which presents bond alternation along the entire backbone. Thus, the protonation of the Schiff base introduces an extra positive charge in the chromophore, which induces a conjugation defect.[21] This defect is localized adjacent to the electronegative nitrogen. Optimization of the structure of the rhodopsin RPSB without a counterion yields qualitatively similar results, but the conjugation defect is more delocalized along the conjugated backbone. The dynamics of this charged defect or soliton has been studied in ref 21.

The structure of the bathorhodopsin RPSB has been obtained starting from the optimized rhodopsin RPSB structure where the hydrogen bound to C12 was flipped into a *trans* position with respect to the hydrogen bound to C11. This initial configuration is highly strained. Indeed, when the system is allowed to evolve in a microcanonical molecular dynamics simulation, the backbone readjusts to release the strain. The system reaches a temperature of ∼300 K in about 35 fs of simulation. During the dynamics, the angle between the two planes formed, for instance, by (C7,C8,C9) and (C13,C14,C15) changes from an initial value of about 40° to 110° in approximately 145 fs. The hinge of this motion is the bond C10−C11. C4, C5, and C6 are also involved in the readjustment, while the other atoms of the ring do not move significantly. The short time scale for the chain readjustment is compatible with the time of formation of the primary photoproduct. After 250 fs of free dynamics, in which the system reaches an equilibrium temperature of 270 K, we have cooled the system according to the annealing schedule: 100, 50, and 10 K for a total simulation time of 200 fs. This procedure yields the equilibrium structure reported in Figure 3. Noticeably, the bowlike structure of Figure 3 is obtained with relatively small atomic displacements from the 11-*cis* configuration. This accounts for the very short time of formation of bathorhodopsin upon *cis*−*trans* isomerization.

The conjugation defect, which is associated with the excess positive charge on the backbone, is much broader in bathorhodopsin and is centered on C9 when the optimization is performed without the counterion (Table 1). This is apparent from the inversion of bond alternation in the tail of the molecule. In fact, the displacement of the conjugation defect results in a bond order inversion, in the fashion of a charged soliton displacement in a conjugated chain.[21] Thus, the bare retinylidene chromophore shows a bistable structure. This is incompatible with the NMR data,[11] which show that no dramatic charge rearrangement occurs when the primary photoproduct is formed. The total energy in the bathorhodopsin model RPSB without the counterion is about 18 kcal/mol higher than in the rhodopsin RPSB.

When the counterion is included in the model, the optimized structure of the bathorhodopsin RPSB presents the charged defect in the terminal region of the tail, in the same position as in rhodopsin (see Table 1). The electrostatic interaction with the counterion locks the conjugation defect in the terminal region of the conjugated system and prevents charge displacement toward the ring, in agreement with experiment.[11]

The computed energy stored in this model bathorhodopsin RPSB including the counterion is ∼22 kcal/mol. The additional energy stored in the system is not related to the charge separation between chromophore and counterion, but rather to greater molecular stiffness. In fact, the interaction with the counterion increases the dimerization of the conjugated chain and prevents charge rearrangement along the backbone, which would decrease the π character of the double bonds and release part of the strain. Thus, the counterion is crucial to the energy storage in our model bathorhodopsin, since it affects the structural properties of the chromophore.

In Table 2 we report the torsional angles for C−C−C−C groups and for H−C−C−H groups on the backbone. The steric hindrance of the methyl group bound to C13 induces an out-of-plane deformation of the chromophore of rhodopsin. In our model of the rhodopsin RPSB, the deformation is distributed along the backbone, rather than being localized on the torsion of a specific bond (Table 2). The torsional angles in the region C9−C14 of rhodopsin present significant deviations from planarity. The total out-of-plane deformation is approximately 40°, but the individual bond twists are small (see also Figure 2b).

The deviations of the torsional angles in the bathorhodopsin RPSB indicate a severe strain in the backbone, which presents the deformed all-*trans* structure of Figure 3b. Noticeably, while the deviations from planarity calculated for the C−C−C−C groups are large, the deviations for the H−C−C−H groups are much smaller. In fact, the distortion includes twists around the bonds as well as bends of the backbone, as apparent from the bowlike structure of Figure 3b. The out-of-plane displacements of the hydrogen atoms are distributed over the chain and are relatively small. This is consistent with the experimental observation that the hydrogen out-of-plane vibrational modes are similar in rhodopsin and bathorhodopsin.[26]

The energy stored in our model of bathorhodopsin is lower than the experimental value. This may be due to an incomplete dimerization in the computed structure of the RPSB. In retinals, similar calculations yield a slightly underestimated dimerization amplitude.[20] Moreover, the energy stored in the chromophore

TABLE 1: Computed Carbon−Carbon Bond Lengths (in Å) for the Optimized Structures of Rhodopsin, Bathorhodopsin, Rhodopsin Including the Cl^- Counterion, Bathorhodopsin Including the Cl^- Counterion, and Unprotonated Schiff Base (SB)

bond	rhodopsin	bathorhodopsin	rhodopsin+Cl^-	bathorhodopsin+Cl^-	unprotonated SB
C5═C6	1.380	1.386	1.370	1.376	1.370
C6−C7	1.439	1.434	1.460	1.445	1.460
C7═C8	1.375	1.387	1.367	1.380	1.367
C8−C9	1.430	1.421	1.442	1.425	1.442
C9═C10	1.399	1.419	1.388	1.402	1.388
C10−C11	1.405	1.390	1.422	1.402	1.422
C11═C12	1.400	1.413	1.389	1.400	1.389
C12−C13	1.413	1.400	1.423	1.407	1.445
C13═C14	1.410	1.424	1.406	1.420	1.378
C14−C15	1.387	1.380	1.391	1.383	1.453
C15═N	1.343	1.357	1.342	1.359	1.294

TABLE 2: Computed Torsional Angles (in deg) along the Backbone for the Optimized Structures of Rhodopsin Including the Cl^- Counterion or Bathorhodopsin Including the Cl^- Counterion; The Sign Follows the Standard Anticlockwise Convention

torsional angle	rhodopsin + Cl^-	bathorhodopsin + Cl^-
C6−C7−C8−C9	+180	+159
C7−C8−C9−C10	−174	−148
C8−C9−C10−C11	−179	+133
C9−C10−C11−C12	−169	−160
C10−C11−C12−C13	+17	+143
C11−C12−C13−C14	−166	+173
C12−C13−C14−C15	+180	−176
C13−C14−C15−N	−178	+179
H-C7−C8−H	−172	+180
H-C8−C9−Me	−179	−172
Me-C9−C10−H	−178	+164
H-C10−C11−H	−165	+166
H-C11−C12−H	+8	+163
H-C12−C13−Me	−154	+161
Me-C13−C14−H	+175	−173
H-C14−C15−H	+180	−176
H-C15−N-H	−176	−167

of bathorhodopsin is likely to depend on the starting RPSB structure and on the counterion structure and distance from the chromophore. In addition, water molecules in the binding pocket and interactions with other protein residues may also play a role. Unfortunately, these details have not been experimentally characterized yet. Nevertheless, the mechanisms described above depend on the fundamental physical properties of the system and are generally applicable.

V. HOMO and LUMO Analysis

Although DFT-LDA calculations underestimate energy gaps, variations of the gaps induced by structural changes are properly accounted for.[29,30] Indeed, while the computed values of the energy gap for rhodopsin (1.42 eV) and bathorhodopsin (1.22 eV) underestimate the experimental values of 2.489 and 2.283 eV, respectively, the calculated energy gap difference between rhodopsin and bathorhodopsin (0.2 eV) correlates well with the experimental value of 0.206 eV.[1]

Moreover, we have computed dipole matrix elements, which are directly related to the transition probability between occupied and unoccupied molecular orbitals and, thus, to the absorption coefficient.[29,30] We find that the HOMO−LUMO dipolar matrix element is the dominant transition, being 1 order of magnitude larger than the other transitions in the visible range.

The HOMO and the LUMO are well separated in energy from the other electronic states, and therefore an analysis of the corresponding electronic densities can be performed. In Figure 4 and Figure 5 we report the HOMO and the LUMO electronic charge densities for the rhodopsin and bathorhodopsin RPSB. A similar analysis for 11-*cis* and all-*trans* retinals is reported in ref 20. In both rhodopsin and bathorhodopsin, the electronic

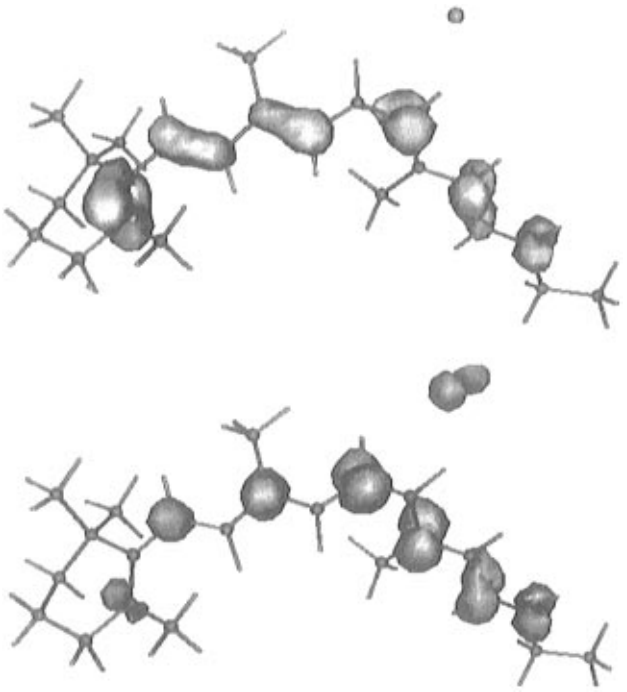

Figure 4. HOMO (a, top) and LUMO (b, bottom) electron charge density distribution in the model chromophore of rhodopsin. The isosurfaces correspond to an electron density of 0.005 e/au^3.

charge of the HOMO is mainly localized on the ring and on the double bonds of the conjugated backbone chain. In the LUMO, the charge is displaced toward the tail. Thus, the photoexcitation corresponds to a sudden polarization inversion by a net transfer of the excess positive charge borne by the chromophore toward the ring. The dynamics of the charge and of the related conjugation defect have been studied in ref 21, where the implications of a soliton-like coherent excitation for the isomerization are discussed.

The HOMOs of both the rhodopsin and bathorhodopsin RPSB reveal a strong π character on the C5═C6 bond, which gradually turns p-like for carbons closer to the terminal nitrogen. The reverse occurs for the LUMOs. It is interesting to compare the HOMO and LUMO of rhodopsin with the corresponding molecular orbitals of the 11-*cis* -retinal.[20] While retinal is a neutral system, the chromophore of rhodopsin has a net positive charge introduced by the protonation of the Schiff base. This extra charge is associated with the conjugation defect discussed in the preceding section. The RPSB and the retinal HOMO charge distributions on the ring side are very similar. On the other hand, large differences occur at the tail end, where the conjugation defect is localized in the RPSB. For instance, the HOMO charge distribution on the C14−C15 bond in the RPSB has π character, while it is a pure single bond in the case of the

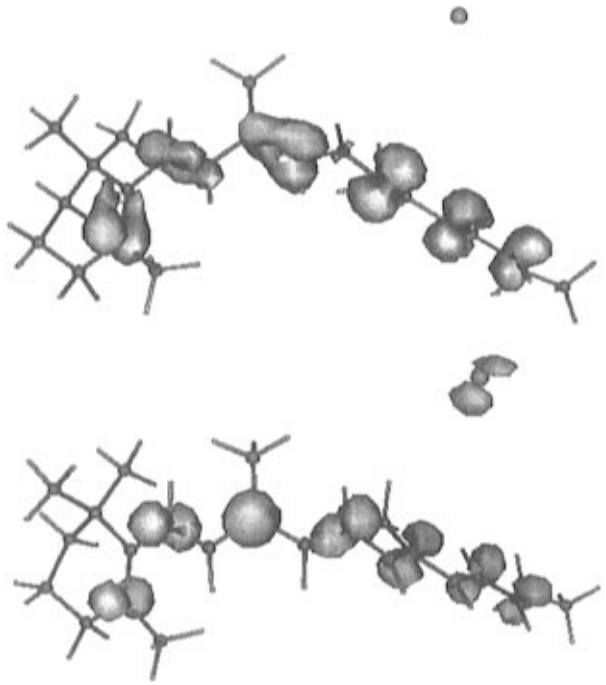

Figure 5. HOMO (a, top) and LUMO (b, bottom) electron charge density distribution in the model chromophore of bathorhodopsin. Same visualization criteria as in Figure 4.

retinal.[20] This correlates with the shorter C14−C15 distance calculated in rhodopsin when compared to the 11-*cis*-retinal.[20]

The comparison between the HOMOs of the bathorhodopsin and rhodopsin RPSB is also very informative, as the charge density differences reflect the deformation of the molecule and their effect on the electronic structure. The π-like lobes corresponding to the twisted bonds present a characteristic deformation, already observed in retinal.[20] For instance, the twist of the C9−C10 bond is reflected in Figure 5a in the charge density, which is wrapped around the bond and spans the twist angle. Correspondingly, the bond length is increased due to the reduced π character induced by the twist (Table 1). The comparison of Figure 4a and Figure 5a shows that in bathorhodopsin the strain is distributed along the entire backbone, in the form of the small bond twists discussed in the former section. These twists are reflected in the increased bond lengths and in the reduced π character of the bond.

The LUMO of the rhodopsin RPSB presents large differences with respect to 11-*cis*-retinal. The charge lobes on the tail are much less pronounced and present less π character. Analogous differences are observed in the LUMO of the bathorhodopsin model.

VI. Conclusion

In conclusion, we have studied the energy storage mechanism in bathorhodopsin, the primary photoproduct of vision, with a Car−Parrinello *ab-initio* molecular dynamics approach. The experimental constraints to the chromophore structure available so far have been included in the model. The excess positive charge borne by the RPSB is associated with a conjugation defect. This defect is located in the terminal region of the rhodopsin and bathorhodopsin RPSB when the electrostatic interaction with the counterion is taken into account. When the counterion is not included in the calculations, a dramatic charge rearrangement occurs upon *cis* to *trans* isomerization, since the defect is displaced toward the ring in the bathorhodopsin RPSB. Thus, the electrostatic interaction with the counterion affects the structural properties of the chromophore. Specifically, it increases the dimerization of the conjugated backbone, increasing the stiffness of the molecule, and prevents the displacement of the conjugation defect. The energy is primarily stored in torsional deformations of the backbone of the bathorhodopsin RPSB. The torsional distortion is distributed over the entire backbone. An analysis of the HOMO and LUMO states in the rhodopsin and bathorhodopsin RPSB has been performed.

Acknowledgment. We wish to thank J. Shelley for the graphics package (MOVIE) used to visualize the results of the simulations. We are grateful to J. Lugtenburg for his constant support and encouragement and to A. Curioni for interesting discussions. We are grateful to M. H. Levitt for a critical review of the manuscript. The numerical calculations were performed in the Computer Center of the Scuola Normale Superiore in Pisa, Italy. The research was partially supported by the EC Biotechnology Program, Contract CT930467. A.B. acknowledges a visiting scientist grant from the Netherlands Foundation for Chemical Research (SON), financed by NWO.

References and Notes

(1) Birge, R. R. *Biochim. Biophys. Acta* **1990**, *1016*, 293.
(2) Lugtenburg, J.; Mathies, R. A.; Griffin, R. G.; Herzfeld, J. *Trends Biochem. Sci.* **1988**, *13*, 388.
(3) Schoenlein, R. W.; Petenau, L. A.; Mathies, R. A.; Shank, C. V. *Science* **1991**, *254*, 412.
(4) Boucher, F.; Leblanc, R. *Photochem. Photobiol.* **1985**, *41*, 459.
(5) Yoshizawa, T.; Wald, G. *Nature* **1963**, *197*, 1279.
(6) Schick, G. A.; Cooper, T. M.; Holloway, R. A.; Murray, L. P.; Birge, R. R. *Biochemistry* **1987**, *26*, 2556.
(7) Cooper, A. *Nature (London)* **1979**, *282*, 531.
(8) Honig, B.; Dinur, U.; Nakanishi, K.; Balogh-Nair, V.; Gawinowicz, M. A.; Arnaboldi, M.; Motto, M. G. *J. Am. Chem. Soc.* **1979**, *101*, 7084.
(9) Warshel, A.; Barboy, N. *J. Am. Chem. Soc.* **1982**, *104*, 1469.
(10) Birge, R. R.; Einterz, C. M.; Knapp, H. M.; Murray, L. P. *Biophys. J.* **1988**, *53*, 367.
(11) Smith, S. O.; Courtin, J.; de Groot, H. J. M.; Gebhard, R.; Lugtenburg, J. *Biochemistry* **1991**, *30*, 7409.
(12) Car, R.; Parrinello, M. *Phys. Rev. Lett.* **1985**, *55*, 2471. Galli, G.; Pasquarello, A. In *Computer Simulation in Chemical Physics*; Allen, M. P., Tildesley, D. J., Eds.; Kluwer: Amsterdam, 1993; p 261.
(13) Verdegem, P.; Bovee-Geurts, P.; de Grip, W.; Lugtenburg, J.; de Groot, H. J. M. Manuscript in preparation.
(14) See, for example: Parr, R. G.; Yang, W. *Density-Functional Theory of Atoms and Molecules*; Oxford University Press: New York, 1989. Jones, R. O.; Gunnarson, O. *Rev. Mod. Phys.* **1989**, *61*, 689.
(15) Perdew, J. P.; Zunger, A. *Phys. Rev. B* **1981**, *23*, 5048.
(16) Ceperley, D. M.; Alder, B. J. *Phys. Rev. Lett.* **1980**, *45*, 566.
(17) Becke, A. D. *Phys. Rev. A* **1988**, *38*, 3098.
(18) Perdew, J. P. *Phys. Rev. B* **1986**, *33*, 8822.
(19) Mintmire, J. W.; White, C. T. *Phys. Rev. B* **1987**, *35*, 4180. Vogl, P.; Campbell, D. K. *Phys. Rev. Lett.* **1989**, *62*, 2012. Ashkenazi, J.; Pickett, W. E.; Krakauer, H.; Wang, C. S.; Klein, B. M.; Chubb, S. R. *Phys. Rev. Lett.* **1989**, *62*, 2016.
(20) Bifone, A.; de Groot, H. J. M.; Buda, F. *Chem. Phys. Lett.* **1996**, *248*, 165.
(21) Buda, F.; de Groot, H. J. M.; Bifone, A. *Phys. Rev. Lett.* **1996**, *77*, 4474.
(22) Vanderbilt, D. *Phys. Rev. B* **1990**, *43*, 7892.
(23) Birge, R. R.; Murray, L. P.; Pierce, P. M.; Akita, H.; Balogh-Nair, V.; Findsen, L. A.; Nakanishi, K. *Proc. Natl. Acad. Sci. U.S.A.* **1985**, *82*, 4117.
(24) Sakmar, T. P.; Franke, R. R.; Khorana, H. G. *Proc. Natl. Acad. Sci. U.S.A.* **1989**, *86*, 8309.
(25) Palings, I.; Perdoen, J. A.; van den Berg, E.; Winkel, C.; Lugtenburg, J.; Mathies, R. A. *Biochemistry* **1987**, *26*, 2544.
(26) Palings, I.; van den Berg, E.; Lugtenburg, J.; Mathies, R. A. *Biochemistry* **1989**, *28*, 1498.
(27) Han, M.; DeDecker, S.; Smith, S. O. *Biophys. J.* **1993**, *65*, 899.
(28) Han, M.; Smith, S. O. *Biochemistry* **1995**, *34*, 1425.
(29) Saitta, A. M.; Buda, F.; Fiumara, G.; Giaquinta, P. V. *Phys. Rev. B.* **1996**, *53*, 1446.
(30) Buda, F.; Fasolino, A. *Phys. Rev. B* **1995**, *52*, 5851.